Lightweight Broadband Antennas for UAV based GPR Sensors

Ralf Burr, Markus Schartel, Winfried Mayer, Thomas Walter, and Christian Waldschmidt

DOI: 10.23919/EuRAD.2018.8546552

Lightweight Broadband Antennas for UAV based GPR Sensors

Ralf Burr[*1], Markus Schartel[#], Winfried Mayer[+], Thomas Walter[*] and Christian Waldschmidt[#]

[*]Laboratory of Microtechnology, Ulm University of Applied Sciences, 89075 Ulm, Germany

[#]Institute of Microwave Engineering, Ulm University, 89081 Ulm, Germany

[+]Endress+Hauser GmbH+Co. KG, 79689 Maulburg, Germany

[1]burr@hs-ulm.de

***Abstract*— In this contribution two different types of broadband antennas namely a logarithmic-periodic dipole antenna (LPDA) and a transversal electromagnetic (TEM) horn antenna for ground penetrating synthetic aperture radar sensors are presented. These antennas are designed to be mounted on an unmanned aircraft vehicle (UAV). The antennas are evaluated in terms of their matching, radiation pattern pulse response and weight. Finally, an integration example of one of these antennas is shown on an UAV.**

***Keywords*— Ground penetrating radar , ultra wideband antennas, dispersion, unmanned aerial vehicles**

I. Introduction

GPRs are a promising technology to detect and classify buried objects such as tubes, pipes and land mines [1]. The detection is not only limited to metallic objects but they are also suitable to determine permittivity differences as they occur during transitions from soil to plastic or other materials.

The electrical properties of the material mainly determine the penetration depth. The main reasons for the penetration depth limitations are material losses, spreading and scattering losses [1]. These losses increase with frequency and thus determine the usable frequency band for the respective application. For mine detection where the ground should be penetrated for several centimeters, the frequency band is limited to a maximum of $5\,\mathrm{GHz}$ [2][3].

Areas which have to be investigated are often not accessible. Due to the ongoing technological progress, small UAVs offer themselves as an autonomous flying carrier platform for GPR sensors. However, these platforms have a restricted payload and the usable mounting area for additional sensors is limited. This forces a trade-off between the lowest usable GPR frequency and the size of the antenna.

In order to separate the reflections of buried objects in the ground, these antennas must have a very high relative bandwidth. For the subsequent processing of the GPR radar measurements, e. g. synthetic aperture radar (SAR), a frequency independence of the antenna characteristics is crucial. In this context in Section II and III, two lightweight broadband antennas are presented. The frequency dependence of their radiation patters are evaluated experimentally. The pulse response of these two antennas is compared in section IV. An integration example of a bistatic antenna configuration on a UAV is shown in section V. Finally a short conclusion is given in section VI.

II. Logarithmic-Periodic Dipole Antenna

The LPDA is a common broadband antenna and can be designed for arbitrary bandwidths. The logarithmic periodic structure was introduced in [4].

The designed LPDA consists of $N = 17$ dipoles in a row. These dipoles differ in size from each other according to the scaling factor $\tau = 0.88$ and vary their distance according to the distance factor $\sigma = 0.16$. The lower cut-off frequency of the antenna is set to $f_u = 1\,\mathrm{GHz}$, thus determining the length of the first dipole to $l_1 = 158\,\mathrm{mm}$. The initial spacing between the first and second dipole is optimized to $s_1 = 25.2\,\mathrm{mm}$.

The antenna is fed via coaxial cable at the position of the smallest dipole of the antenna. In order to maintain the symmetry characteristic of the antenna the same cable has also been installed on the back side. The antenna was manufactured on a $1\,\mathrm{mm}$ thick low cost FR4 substrate with a relative dielectric constant $\varepsilon_r = 4.3$. The manufactured antenna is shown in Fig. 1 and weighs $63\,\mathrm{g}$.

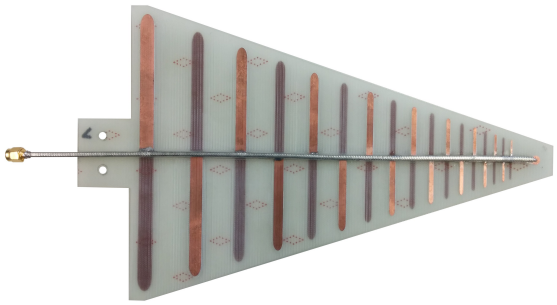

Fig. 1. Manufactured logarithmic periodic dipole antenna with $\tau = 0.88$ and $\sigma = 0.16$.

Simulation and Measurements

The matching and pattern of the antenna is simulated and optimized. The comparison between measurement and simulation is shown in Fig. 2.

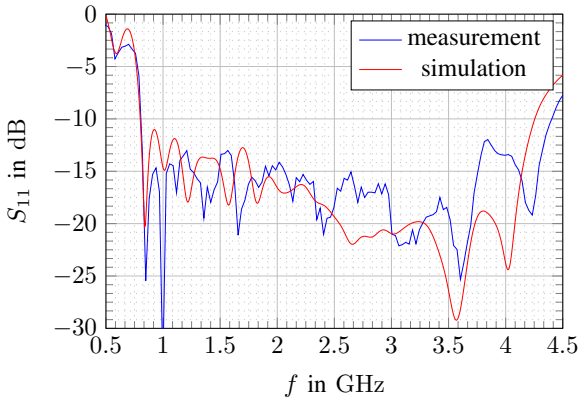

Fig. 2. Comparison of the matching between simulation and measurement in the frequency range from 0.5 GHz to 4.5 GHz.

Fig. 2 shows a good agreement between simulation and measurement. The differences of individual resonance frequencies are due to the not exactly known permittivity and deviating homogeneity of the substrate.

Fig. 3 shows the antenna pattern of the LPDA over frequency. The constant lobe width is in the E- and H-plane over frequency clearly visible. As expected, the beam width in the E plane is approximately 64° and in the H plane 110°.

III. TEM-Horn Antenna

The transversal electromagnetic horn antenna or TEM-horn antenna is a travelling wave antenna. It consists of two opposite metal plates with a gradually increasing spacing. In order to achieve a good matching of the feed to the horn funnel, this expansion must be continuous and slow. This can be done in a linear or exponential manner [5]. An exponential opening is used for the manufactured antenna. The advantages of an exponential opening is the three times higher bandwidth at the same antenna size compared to a linear opening [6].

The horn funnel expands according to the following exponential function:

$$y(x) = A_1 e^{C_1 x} + B_1 \tag{1}$$

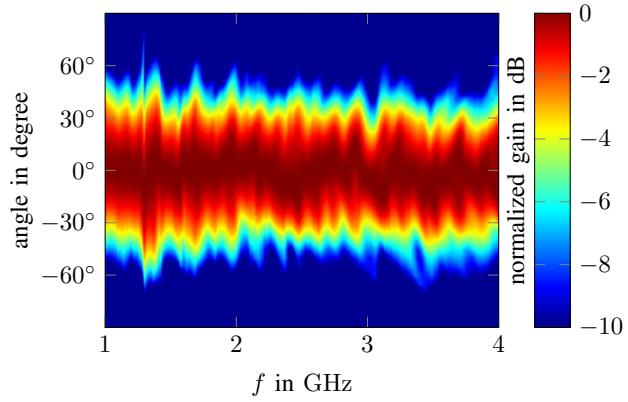

(a) E-plane

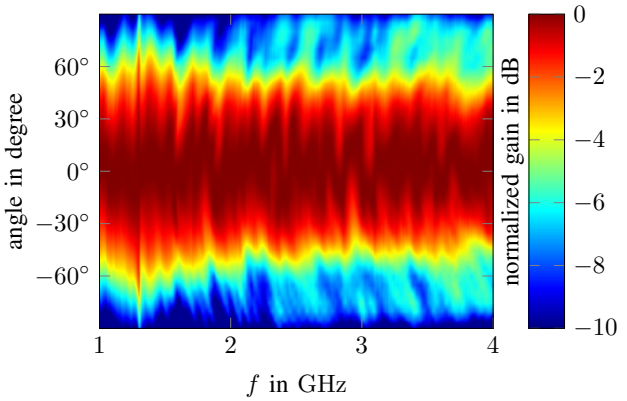

(b) H-plane

Fig. 3. Antenna pattern of the LPDA over the frequency range 1 GHz to 4 GHz.

The calculations of the coefficients A_1 and B_1 can be done with the help of the length L, the initial plate spacing d at the feeding point and the final opening width D at the end of the horn and are shown below [7]:

$$A_1 = \frac{\frac{W}{2} - \frac{d}{2}}{e^{C_1 L} - 1} \tag{2}$$

$$B_1 = \frac{\frac{d}{2} e^{C_1 L} - \frac{W}{2}}{e^{C_1 L} - 1} \tag{3}$$

The width of the horn funnel also opens according to an exponential function. For modeling the z-axis equation (4) is used. The coefficients A_2 and B_2 are calculated according to the initial width w_{feed} and final width W of the exponential horn funnel with formula (2) and (3).

$$z(x) = A_2 e^{C_2 x} + B_2 \tag{4}$$

The degrees of freedom of the two exponential apertures are C_1 and C_2. This parameter has been simulated and optimized. The exponential opening shows that several modes occur at higher frequencies and the main lobe splits. To avoid this a rounding at the end of the horn funnel is suggested in [8]. The transition of the rounding is designed in such a way that the bend of the curve at the end of the exponential funnel is the same as in the rounding. This rounding increases the horn aperture from D to the width D_2. The width is also designed to increase the opening linearly from W to W_2.

The optimized parameters for the exponential opening coefficient and best matching in the frequency range 1 GHz to 4 GHz are $C_1 = 0.019\,98$ and $C_2 = 0.011$. The design parameters are shown in Table 1.

Table 1. Optimized model parameters of the TEM-horn antenna.

C_1	C_2	W	W_2	D	D_2	d	w_{feed}
0.01998	0.011	170*	190*	130*	210*	2.6*	7.5*

*all dimmensions in mm.

In order to keep the antenna as light as possible, the conductive surfaces are made of a $0.05\,\mathrm{mm}$ thick copper foil. The exponential progression of this film is achieved with a printed acrylonitrile butadiene styrene (ABS) support structure. This structure has a honeycomb-shaped infill which makes it very lightweight and stable. The infill of the structure corresponds to $10\,\%$ of the volume which has also a neglectable influence to the radiation characteristics of the antenna. The feeding at the end of the antenna is made of two opposite $0.3\,\mathrm{mm}$ thick copper sheets which have a capacitive transition to a coaxial connector. The manufactured antenna is shown in Fig. 4.

Fig. 4. Manufactured TEM-horn antenna.

The total weight of $180\,\mathrm{g}$ of the antenna is composed of functional and construction-related contributions as shown in Table 2.

Table 2. List of the weight contributions of the TEM-horn antenna.

support structure	feed with coax connector	copper foil	adhesive
125 g	12 g	40 g	3 g

Simulation and Measurement

The reflection coefficient with the optimized TEM-horn antenna is shown in Fig. 5. In the frequency range from $0.7\,\mathrm{GHz}$ to $6\,\mathrm{GHz}$ the reflection coefficient is better than $-12\,\mathrm{dB}$. In a range from $1.8\,\mathrm{GHz}$ to $6\,\mathrm{GHz}$ the reflection coefficient is better than $-17\,\mathrm{dB}$. Comparing the simulations to the measurement results a good correlation between the resonance frequencies and the bandwidth can be seen.

The frequency dependence of the antenna pattern of the E- an H-planes is shown in Fig 6. The H-plane shows an expansion of the main lobe in the range from $1\,\mathrm{GHz}$ to $0.5\,\mathrm{GHz}$ and in the range of $3\,\mathrm{GHz}$ which is caused by the finite antenna aperture.

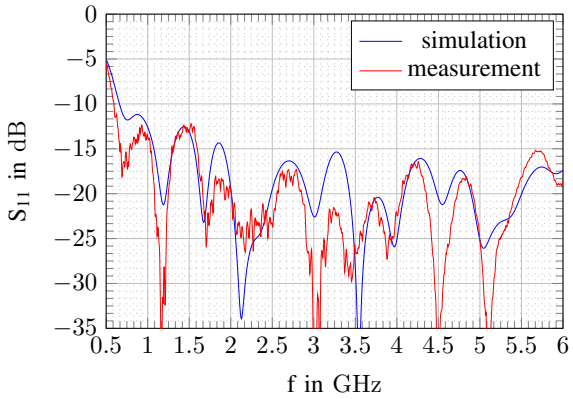

Fig. 5. Comparison of the matching of the TEM-horn antenna between simulation and measurement.

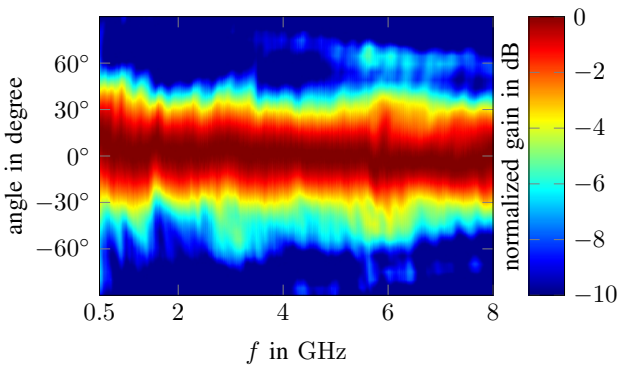

(a) E-plane

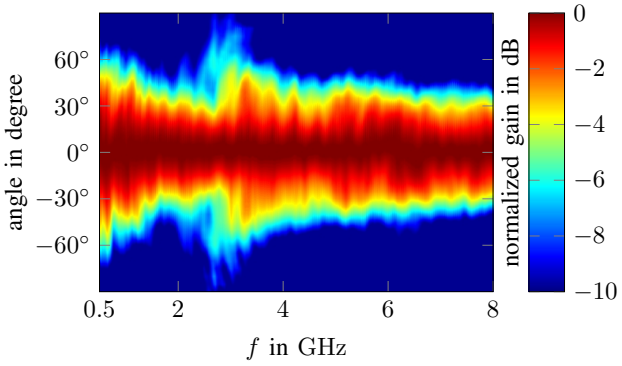

(b) H-plane

Fig. 6. Antenna pattern of the TEM-horn over the frequency range $0.5\,\mathrm{GHz}$ to $8\,\mathrm{GHz}$.

IV. Pulse Response Comparison

Due to the large dimension relative to the center frequency of such broadband antennas the phase center of the antenna moves with the frequency. This leads to a distortion of the impulse response of the antenna which can not be neglected for SAR processing. Depending on the radar system this distortion can be removed or not. If the radar does not have an angular resolution the dispersion correction can be performed without

further effort for a fixed angle. Fig. 7 shows the pulse response of the two antennas. The pulse response of the LPDA as shown in Fig. 7b is spread over the entire length of the antenna. This distortion is not visible for the TEM-horn antenna.

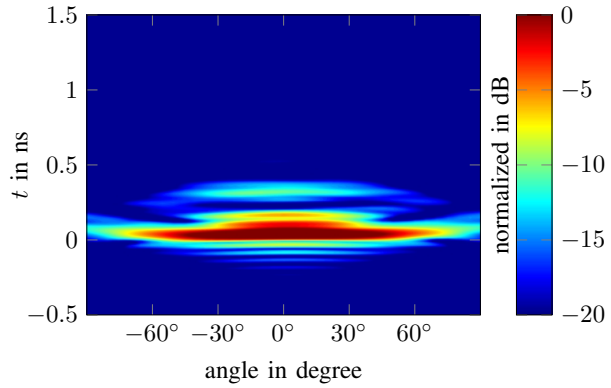

(a) TEM-horn antenna

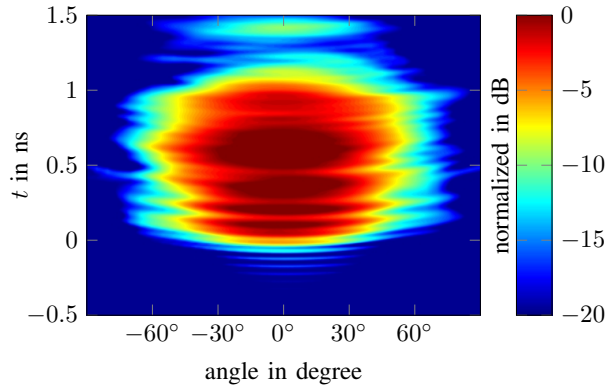

(b) LPDA

Fig. 7. Two way pulse response for the frequency range 1 GHz to 4 GHz in the E-plane.

V. UAV Integration

The in-house developed radar works in a bistatic configuration in the frequency range from 1 GHz to 4 GHz [9]. Due to the pulse response two TEM-horn antennas were used on a DJI M600 Pro UAV which provides a carrier platform with a payload of up to 6 kg. The antennas are suspended from a carbon tube and take up 400g of the payload including attachments. The flight platform with both antennas is shown in Fig. 8.

VI. Conclusion

In this contribution a LPDA and a TEM-horn antenna is simulated, manufactured and characterized. In the frequency range 1 GHz to 4 GHz, they provide an almost frequency independent radiation pattern. With 60 g, the LPDA is very light and suitable for UAVs. The planar structure also has a low construction volume and low wind load in one direction which is important for mounting on a UAV.

Fig. 8. Photo of the carrier platform DJI M600 Pro equipped with two TEM-horn antennas.

With 180 g , the TEM-horn antenna is about three times heavier than the LPDA.The construction volume of the antenna is also much larger but has a much more focused antenna pattern in the H-plane. The side walls of the TEM-horn antenna are also open which reduces the wind load.

Comparing the pulse response of the two antennas it can be seen that the LPDA distorts the pulse to its full length. This distortion cannot be corrected for pulsed radars. For radars in the frequency range, such as a FMCW radar, the correction is possible but only for one spatial direction.

Acknowledgment

The authors thank the Urs Endress foundation for supporting this work (https://www.ue-stiftung.org).

Part of the measurement equipment was founded by the BMBF in the projekt Terasens.

References

[1] D. Daniels, *Ground Penetrating Radar*, ser. Electromagnetics and Radar Series. Institution of Engineering and Technology, 2004, no. Bd. 1.

[2] C. Fischer and W. Wiesbeck, "Multistatic gpr for antipersonnel mine detection," in *IGARSS 2001*, vol. 6, 2001, pp. 2721–2723 vol.6.

[3] M. Fritzsche, *Anwendungen von Verfahren der Mustererkennung zur Detektion von Landminen mit Georadaren*. Universitt Karlsruhe, 2001.

[4] D. Isbell, "Log periodic dipole arrays," *IRE Transactions on Antennas and Propagation*, vol. 8, no. 3, pp. 260–267, May 1960.

[5] M. Khorshidi and M. Kamyab, "New exponential TEM horn antenna with binomial impedance taper," *International Journal of Electronics and Communications*, vol. 64, no. 11, pp. 1073 – 1077, 2010.

[6] J. Wang, C. Tian, G. Luo, Y. Chen, and D. Ge, "Four element TEM horn array for radiating ultra-wideband electromagnetic pulses," *Microwave and Optical Technology Letters*, vol. 31, no. 3, pp. 190–194, 2001.

[7] Z. Wang and X. Xie, "Design and optimization of the antenna applied for detecting the voids in tunnel lining by gpr," in *Ground Penetrating Radar (GPR), 2012 14th International Conference on*, June 2012, pp. 131–136.

[8] M. Abbas-Azimi, F. Arazm, J. Rashed-Mohassel, and R. Faraji-Dana, "Design and optimization of a new 1 to 18 GHz double ridged guide horn antenna," *Journal of Electromagnetic Waves and Applications*, vol. 21, no. 4, pp. 501–516, 2007.

[9] R. Burr, M. Schartel, P. Schmidt, W. Mayer, T. Walter, and C. Waldschmidt, "Design and implementation of a FMCW GPR for UAV-based mine detection," in *2018 IEEE MTT-S International Conference on Microwaves for Intelligent Mobility (ICMIM 2018)*.